3 Experimental methods

> "Nothing tends so much to the advancement of knowledge as the application of a new instrument. The native intellectual powers of men in different times are not so much the causes of the different success of their labours, as the peculiar nature of the means and artificial resources in their possession."
>
> — Sir Humphrey Davy
>
> in: Thomas Hager, *Force of Nature,* Simon and Schuster, New York, 1995, p. 86.

In order to study the electrode/electrolyte interface in situ, we employed the quite recently developed Surface Plasmon Resonance (SPR) measurements as well as a traditional electrochemical method, namely cyclic voltammetry (CV).

3.1 Surface plasmon resonance measurements

3.1.1 Surface plasmon resonance (SPR)

A plasmon is the quantum of a charge density wave. Charge density waves are collective motions of a large number of electrons in matter. They may arise when electrons are disturbed from their equilibrium state. For example, they can be excited when fast electrons are passed through a thin aluminum foil. When plotting the number of transmitted electrons against their energy loss, each energy-loss peak corresponds to the excitation of one or more plasmons. Within the experimental error, the peaks occur at integral multiples of a fundamental loss. Such a fundamental loss is donated to a plasmon (one quantum) [42].

Surface plasmons (SPs) are charge density waves that are confined to the surface of a metal or, more precisely, the interfacial region between a metal and a dielectric medium, such as vacuum, air or a liquid. Their excitation (Surface Plasmon Resonance (SPR)) can be achieved by a quantum optical-electrical process, i.e., by the irradiation with photons.

The prerequisite of the excitation of SPs by light is that the energy carried by the photons can be "coupled" or transferred to the electrons of the metal. This is

possible if the metal possesses conduction band electrons and these electrons can resonate with light in the appropriate conditions. With a variety of metals such an excitation of SPs is possible. Among these metals, gold is the most suitable one for the experimental studies carried out by SPR measurements. Other metals are either quite expensive (In), violently reactive (Na), too broad in their SPR response (Cu, Al), or too susceptible to oxidation (Ag).

Surface plasmons, i.e., the charge density wave, propagate along the interface. Their electric field vectors possess their maxima at the interface and decay exponentially perpendicular to the interface into both media (Fig. 3.1).

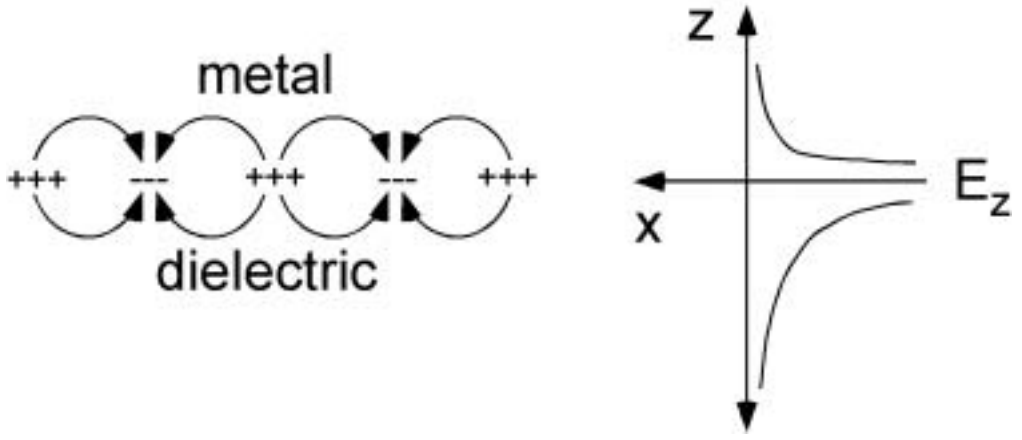

Figure 3.1: *Schematic of surface plasmon waves at the interface between a metal and a dielectric. The plasmon propagates into the x-direction and it decays exponentially into the z-direction.*

Some major characteristics of surface plasmons at the metal/water interface are compiled in Table 3.1.

Table 3.1: *Major characteristics of surface plasmons at the metal/water interface [43].*

Metal layer supporting SPs	Silver		Gold	
Light source wavelength	630 nm	850 nm	630 nm	850 nm
Propagation length (μm)	19	57	3	24
Penetration depth into metal (nm)	24	23	29	25
Penetration depth into dielectric (nm)	219	443	162	400
Concentration of field in dielectric (%)	90	95	85	94

The principle of the excitation of SPs by light

It is not possible to excite SPs by irradiating a metal surface directly by light. In such a configuration photons cannot couple to SPs. This can be understood with the help of the dispersion curve of the SP (a plot of SP frequency versus SP wave vector) [44]. In the following the derivation of the dispersion relation is outlined thoroughly (for an extensive treatment of the problem, see, e.g., the book [45]).

Consider a metal that is in contact with a dielectric medium. Setting the outer normal to the metal surface as +z-direction, the charge density produced by the surface electrons is given by [46]:

$$\rho(x,z,t) = \rho_0 \exp[i(k_x x - \omega t)]\exp(qz) \qquad (3.1)$$

with

$$q = [k_x^2 - \alpha(\omega^2 - \omega_p^2)]^{1/2}, \qquad (3.1a)$$

where ω_p is the plasma frequency, and $\alpha = (\frac{3}{5}\upsilon_F^2)^{-1}$, v_F is the Fermi velocity of the electrons.

The coupled transverse electric fields inside (-) and outside (+) the solid are described by:

$$E^{\pm}(x,z,t) = E_0^{\pm} \exp[i(k_x x - wt)]\exp(k^{\pm} z) \qquad (3.2)$$

with

$$k^{+} = -[k_x^2 - (\omega/c)^2 \varepsilon_s]^{1/2}, \tag{3.2a}$$

$$k^{-} = [k_x^2 - (\omega/c)^2 \varepsilon_m]^{1/2}. \tag{3.2b}$$

Here ε_m stands for the complex dielectric function of the metal, and ε_s is the ambient dielectric constant. The electric field of the SP represents a harmonic wave along the surface (x, y-plane) with frequency ω and wave vector k_x, while perpendicular to the surface (z-direction) the fields are exponentially decaying. Thus, $\left|k^{+}\right|$ is a measure of the penetration depth of the SP into the adjacent medium. Since $\alpha^{-1/2}$ is of the order of the Fermi velocity υ_F, we find $q >> k^{\pm}$ (about a factor of c/υ_F) for $\omega \le \omega_p / \sqrt{2}$, while k_x is of the order of (ω/c). Hence, the charge density perturbation (Eq. (3.1)) decays much faster than the transverse fields (Eq. (3.2)) and we can therefore approximate the charge perturbation at the surface by a δ function as done in standard optics. This allows us to treat SP waves by classical optics, and we can derive their dispersion relation from the usual boundary conditions:

$$\varepsilon_s k^{-} - \varepsilon_m k^{+} = 0. \tag{3.3}$$

Inserting Eqs. (3.2a) and (3.2b) into Eq. (3.3) leads to the more explicit form of the SP dispersion relation (for $\omega < \omega_p$) [47]:

$$k_x = \left(\frac{\omega}{c}\right)\left(\frac{\varepsilon_s \varepsilon_m}{\varepsilon_s + \varepsilon_m}\right)^{1/2}. \tag{3.4}$$

Note, however, that ε_m (and in principle also ε_s) are frequency dependent quantities. A dispersion relation for SPs at the metal/vacuum interface (ε_s = 1) in which ε_m has been approximated by the Drude dielectric function of a free electron gas (see, e.g., the book [45], p. 237) is shown in Fig. 3.2 (k_{sp} curve). In addition, the linear dispersion relation for photons in vacuum is depicted by the dashed line (k_0 curve). Clearly, the two dispersion relations do not have any nontrivial intersection, and thus SPs cannot be resonantly excited under these conditions.

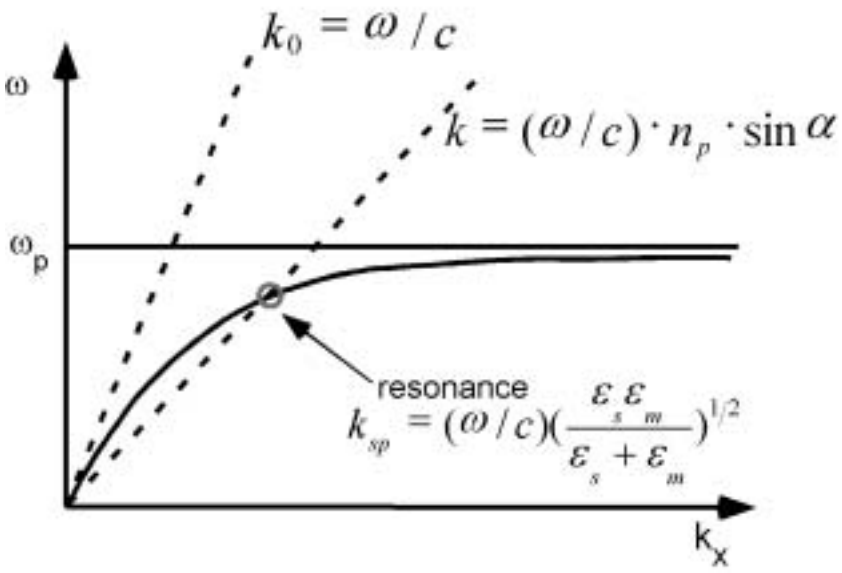

Figure 3.2: *Dispersion relation of surface plasmons and light traveling through vacuum and through a medium with refractive index n_p.*

The coupling of photons and SPs becomes possible if they possess the same wave vector k_x for a given frequency w. In other words, the two dispersion curves should intersect. From Fig. 3.2 it is apparent that this will be the case if the slope of the dispersion curve of the photons (*k* curve, dashed line), which is equal to the speed of light, is decreased. Decreasing the speed of light is possible by passing it through a medium with a larger refractive index. This illustrates why SPs can be excited in the so-called 'Kretschmann configuration' [48].

In the Kretschmann configuration (another well-known configuration is the Otto configuration, for a description see, e.g., [47]) the metal is a thin film (e.g., a 50 nm thick Au film) which is on one side in contact with a dielectric medium of high refractive index (most often a glass) and on the other side with a second dielectric medium, which might be a vacuum, or, as in our experiments, an aqueous electrolyte (Fig. 3.3). Passing a light beam through the high-refractive medium, surface plasmons can be excited in the metal film. (Note that in this configuration the quantitative dispersion relation depends on the refractive indices of all three phases and is thus somewhat more complicated than in the above considered case.)

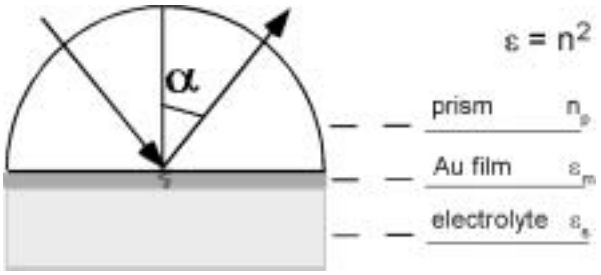

Figure 3.3: *Kretschmann configuration.*

In practice, a laser beam, i.e., light with a well defined wavelength, is used. Hence, the excitation of SPs can occur if

$$K_{para} = K_{sp}, \tag{3.5}$$

where

$$K_{para} = n_p(\frac{2\pi}{\lambda_0})\sin\alpha \tag{3.5a}$$

is the component of the electric wave vector of the photons in the metal surface and K_{sp} the wave vector of the surface plasmons. n_p is the refractive index of the prism, λ_0 the wavelength of incident light, α the incidence angle, ε_m the dielectric constant of the metal, ε_s the dielectric constant of the electrolyte. Hence, clearly, in the Kretschmann configuration, the resonance condition is fulfilled only for a specific angle of incidence, α. In addition, only the component of the electric field of photons that is parallel to the plane of incidence, can excite SPs. Thus, in the experiments p-polarized light is used. S-polarized light, i.e., light, whose electric field vector is perpendicular to the plane of incidence, is totally reflected at the prism/metal interface.

The value of SP excitation in an electrochemical environment results from the fact that the resonance condition depends sensitively on the optical properties of

the interfacial region between metal and electrolyte. Changing the electrode potential changes the charge on the metal surface and also the composition of the double layer. It might also lead to the adsorption of species from the electrolyte on the surface. Both processes change the dielectric constant of the interfacial region, whereby adsorption has in general a larger effect than changes of the charge (and thus the concentration of counter ions in the double layer). Thus, monitoring the resonance angle during a potential scan yields information on changes in the electrode coverage or double layer concentration, as demonstrated by various groups [44, 48-50] two decades ago.

More recently, surface plasmon resonance was also exploited in order to obtain a spatially resolved picture of the optical properties of the electrode, and thus, e.g., the lateral distribution of adsorbates.

In this thesis, both types of measurements were employed, surface plasmon resonance angle measurements (SPRA) and surface plasmon imaging (SPI). The corresponding setups are described in the following two sections.

3.1.2 Surface plasmon resonance angle measurement (SPRA)

One advantage of the SPR measurement is that it is an in-situ method, i.e., the measurement can be done without interfering with other reaction processes during an electrochemical experiment. In a conventional setup, the electrode potential is fixed at a certain value and the intensity of the reflected laser beam is measured as a function of the angle of incidence. Once the desired range of incidence angles is scanned, the electrode potential is set to the next value and the angle of incidence is scanned again. In this way, only slow changes can be followed.

In our experiments we realized a different setup that is briefly mentioned in [44]. Its advantage is that the temporal resolution is much higher. Before entering the prism, the laser beam was first expanded and then focused onto the gold film. In this way, a whole range of angles of incidence is reflected instantaneously. At those values of the angle of incidence, at which SPs are excited, the reflected

intensity is minimal. Hence, measuring the profile of the reflected p-polarized light yields an intensity curve from which the resonance angle can be determined (Fig. 3.4).

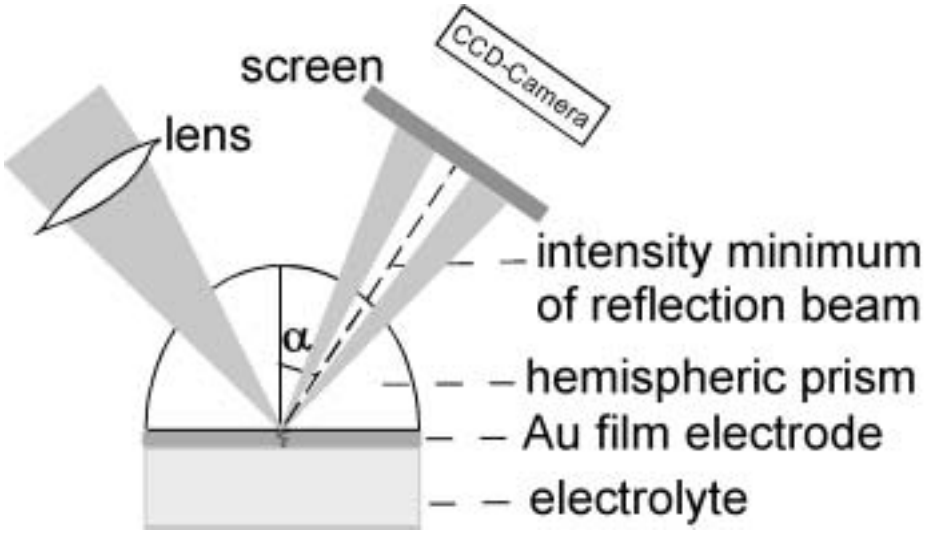

Figure 3.4: *Setup of the SPRA measurement.*

Due to the Gaussian profile of the laser beam as well as to optical imperfections of the setup, the minimum position can be distorted in the measurement. To minimize the distortion, we determined also the profile of a reflected s-polarized laser beam and normalized the intensity of the reflected p-polarized curve to the s-polarized one.

Examples of the intensity curves obtained with s- and p-polarized light are depicted in Fig. 3.5. Before each experiment, we first recorded one intensity curve with s-polarized light, then started the electrochemical experiment (e.g., measured a cyclic voltammogram) and in parallel recorded the intensity of the reflected p-polarized laser beam. After a complete CV was recorded in this way, all p-polarized intensity curves were normalized to the one obtained with s-polarized light. Then the minimum position of each normalized profile was determined yielding the evolution of the SPR angle as a function of time, and

thus, in the case of a potential scan, also of the potential. The determination of the minimum position was done in two steps. First a polynomial of the 5th degree was fitted to the normalized curve around the minimum position, and then the minimum of the fitted curve was determined by determining the root of the differentiated fit function.

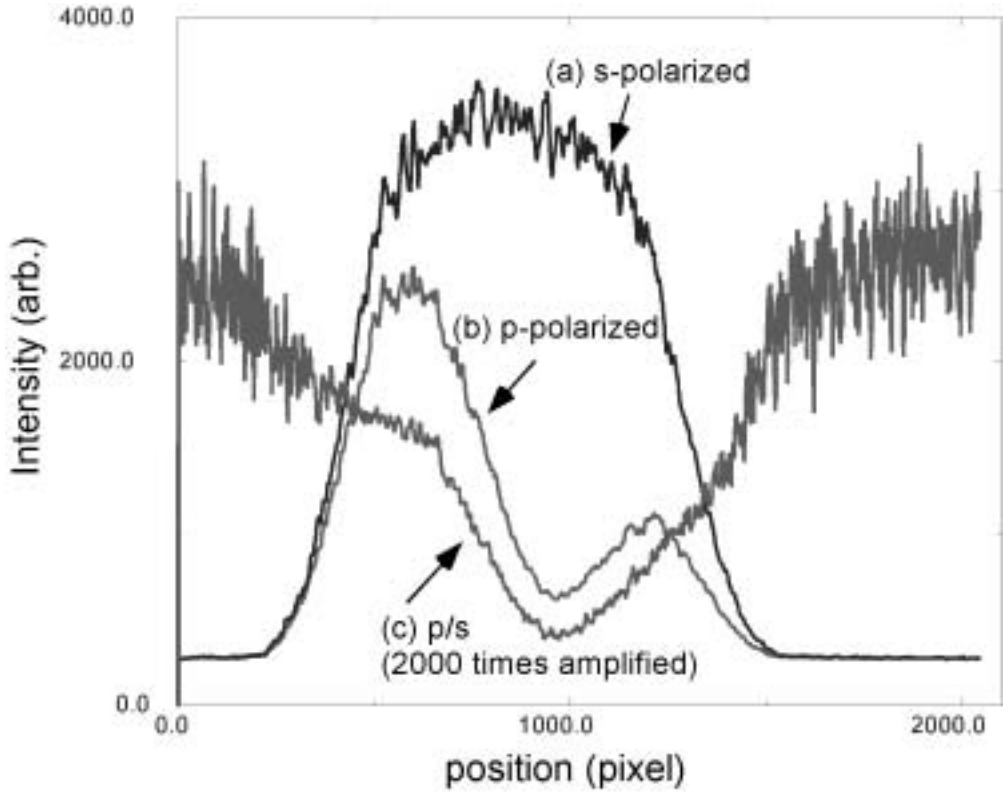

Figure 3.5: *(a) and (b), curves of horizontal light intensity distribution on the screen from s- and p-polarized laser beams, respectively; (c), the curve obtained by normalizing (b) curve to (a) curve (amplified 2000 times).*

In all described experiments a He-Ne laser with a wavelength of 632.8 nm was used. The coherence of the laser light was destroyed by passing it through two rotating glass plates that fixed a sheet of greaseproof paper (see below). Behind them a polarizer reestablished linear polarization and a λ/2 plate allowed an easy switching between s- and p-polarization. With several lenses the laser beam was

first broadened and then focused onto the electrode. The reflected light was made visible by putting a screen into the optical path of the reflected beam. The intensity profile on the screen was recorded with a Line Scan Camera (703 E, Vistek) with 2048 pixels in which the standard 8bit ADC was exchanged by a 12 bit ADC. The optical data were stored simultaneously with current and potential during a potentio-dynamic experiment. The prism was a section of a hemisphere (BK 7, Schott, Germany, polished to $\lambda/10$ by B. Halle Nachfl. GmbH) which allowed to focus the laser beam onto the working electrode. With a 'normal' prism (as used for surface plasmon imaging) a 'point-like' focus cannot be obtained. The working electrode was evaporated onto a glass plate (B270 Schott, Germany polished by B. Halle Nachfl. GmbH) which was brought into optical contact with the 'hemisphere prism' with an immersion oil. The preparation of the Au electrode is described in section 3.2.2.

3.1.3 Surface plasmon imaging (SPI)

Surface plasmon imaging (SPI) exploits – just as SPRA measurements do – the extreme sensitivity of the surface plasmon resonance with respect to small changes of the dielectric constant of the interfacial region. However, instead of determining the resonance angle for certain experimental conditions, the intensity is simultaneously measured for a given angle of incidence over a large portion of the electrode. This is realized by generating a broadened parallel laser beam with which the whole electrode, or at least a larger portion of the electrode, is irradiated at a certain angle of incidence, which for optimal contrast should be close to the steepest change of the resonance curve. Then the irradiated part of the electrode is imaged onto a screen. In this way, an intensity pattern is obtained on the screen which reflects the spatial variations of the dielectric constant at the electrode/electrolyte interface: Clearly, when the electrode/electrolyte interface is characterized by a homogeneous dielectric constant, the reflected intensity should also be homogeneous. In contrast, in the case of lateral changes in composition of the double layer or the coverage of the electrode, the resonance condition differs laterally, and some portions of the electrode reflect most of the incident light (no SPs are excited), others absorb it nearly completely. Thus, with a CCD (charge coupled device) with a two-dimensional photodiode array a two-

dimensional image of the potential distribution in front of the electrode or the adsorbate coverage of the electrode can be recorded. This principle is illustrated in Fig. 3.6.

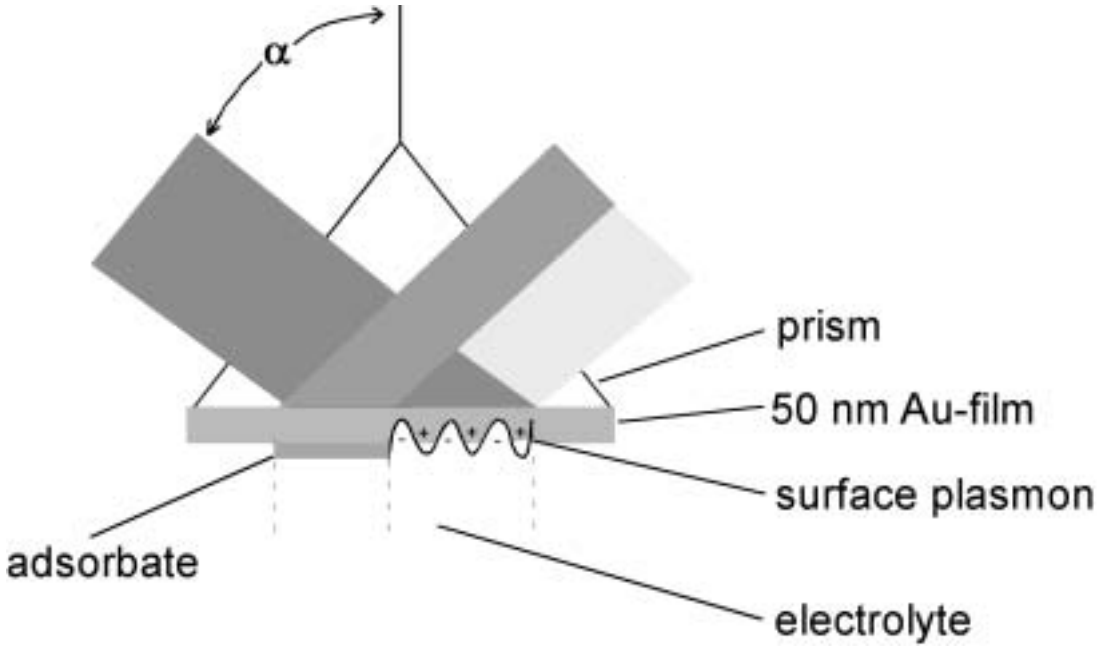

Figure 3.6: *Schematic of the SPR imaging setup.*

The entire experimental setup used in SPI is shown in Fig. 3.7 (included the polarizer and the other lenses, the wavelength of the He-Ne laser is 632.8 nm). From Table 3.1 it can be seen that this choice (at least theoretically) allows us to obtain a spatial resolution of 3 μm. Since the coherence of the laser leads to interference patterns at any 'imperfection' in the optical path, which would then be superimposed to the wanted image of the interface, the coherence of the laser was destroyed by passing the beam through a 'coherence scrambler' before illuminating the electrode. Two different coherence scramblers were employed.

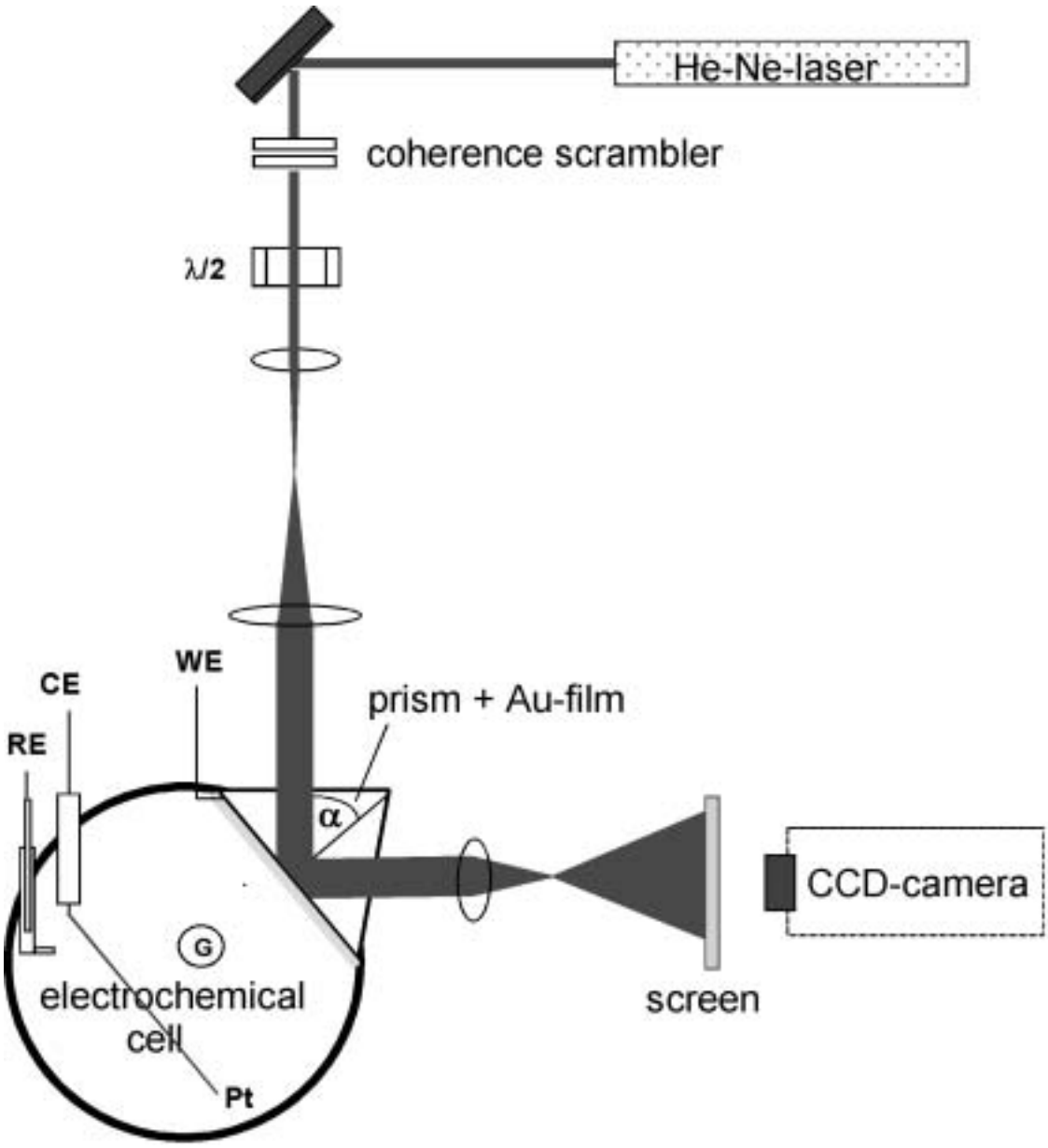

Figure 3.7: *Top view of the electrochemical cell and the setup for surface plasmon imaging. WE, working electrode; RE, reference electrode; CE, counter electrode; and G: gas inlet for bubbling.*

Method A (also used in SPRA): The laser beam was coupled into a glass fiber, whereby care had to be taken that the end of the glass fiber had a 'good', i.e., smooth, section. This was achieved by first heating some location of the fiber with a butane gun until some cracks appeared in the fiber and then, pulling the

fiber horizontally with two hands until it broke. The quality of the section was checked by inspecting the profile of the laser beam that had passed through the fiber. A circular, homogeneous profile without any other patterns ensured that the quality of the section was sufficient. Once a fiber with smooth sections was obtained, it was rolled into innumerous circles with different diameters. This bundle of fiber circles was then fixed onto a stick, which was connected to the vibrating part of a speaker. In this way, all the fiber cycles are vibrating with the speaker in a certain frequency, and the coherent character of the laser light is thus reduced. The efficiency of the reduction depended on the frequency and amplitude of the vibration of the speaker. Both had to be finely tuned for good results. Adjusting the fibers turned out to be very time consuming. Therefore, in the second half of this thesis, another coherence scrambler was set up.

Method B (also used in SPRA): This second way employed to destroy the coherence of the laser light is to use "rotating plates", i.e., two transparent disk shaped glass plates (thickness about 5 mm, diameter about 10 cm), between which a sheet of greaseproof paper was fixed and which were mounted to the axis of a motor. The laser beam was passed through several lenses and was focused to the middle of the layer of the plates. The rotation of the plates destroyed the coherence of the laser beam, leading in general to a homogeneous laser beam section.

Behind the coherence scrambler a lens with its focus in the middle layer of the plates led again to a parallel beam. A polarizer was used to reestablish linear polarization, and a $\lambda/2$ plate allowed to adjust the polarization easily. Finally, before entering the prism, the beam was broadened once more with a combination of a 15 mm and a 300 mm lens. The lenses were put in a distance of 31.5 cm such that the beam remained parallel. In this way, the beam was expanded by a factor of 20. The middle part of the beam was then used for surface plasmon imaging.

With a lens put into the reflected beam, the irradiated electrode was imaged to a screen from where the image was filmed with a Dalsa CCD with a 128 x 128 photodiode array). A temporal resolution of up to 800 frames per second was

achieved with the use of a full-frame transfer architecture, which was connected to an image processing board. In parallel to the images, current and voltage were sampled with a 16 bits A/D converter. The memory of the CCD could store 256 images. The sampling of the images was done continuously in a 'ring', i.e., the oldest images were continuously replaced until the camera received a trigger. The trigger acted as a '50 % pre-trigger', i.e., the 128 last images were stored before the trigger signal and the other 128 images after the trigger signal.

In general, an individual image as recorded was distorted, owing to the Gaussian laser profile and other optical imperfections in the path that resulted in a position-dependent illumination intensity. To observe an image of the optical properties of the electrode/electrolyte interface, the images had to be processed. The following procedure turned out to be best suited: For each pixel the maximum and minimum intensities within a series of images were determined. If the difference exceeded a preset value, which represented the noise level, the intensity interval was stretched to 8 bits (i.e., 256 in decimal unit), otherwise it was set to 0. In this way, differences in the illumination were eliminated without enhancing the noise. Subtracting a 'base image' or taking the differences of successive images gave similar results, but with a lower dynamics.

To process the images in the described way, it was necessary that within the series of recorded images the patterns, i.e., the SP resonance conditions, changed sufficiently. Hence, for the recording of the stationary structures it was necessary to either sample the images during a potential scan that covered a sufficiently large voltage interval such that the pattern changed sufficiently, or to make a potential jump into the pattern forming region from a region where the electrode was homogeneous (cf. section 5.1.2). In practice, when we fixed the potential at a certain point and measured the images with the SPI method, if there is no big change of the surface plasmon resonance conditions, we normally could only observe a homogeneous image even though the electrode is patterned, i.e., we could not measure the unchanging states with our above treatment. In order to increase the contrast of patterns, we usually sampled the images during the potential scan or started at a different potential and then jumped to the potential we are interested in.

3.2 Electrochemical cell and cyclic voltammetry

Cyclic voltammetry is a basic method in electrochemical analysis. For example, it is used to study the electrochemical reactivity of a material, to measure the redox potential, and to investigate the reversibility and the mechanism of an electrochemical reaction, etc. In this thesis it was employed for 1) controlling the quality of the WE, 2) as an indicator for the presence of a first-order phase transition of an adsorbate, and 3) characterizing the reactivity of the adsorbate covered and bare Au electrode with respect to different redox reactions.

The main electronic device employed in a cyclic voltammetric experiment is a potentiostat, which can control the potential difference between the WE and the RE. The potentiostat used in the experiments was designed and produced by the Electronic Laboratory of the Fritz-Haber-Institute (FHI-Elab).

3.2.1 Electrochemical cell

The electrochemical cell we used is a three-electrode one-compartment glass cell. The geometry of the cell was cylindric with the inner diameter of about 6 cm and an approximate height of 5 cm. The top of the cell possessed five tube openings through which the reference electrode (RE), the counter electrode (CE) and the gas in- and outlets could be easily assembled. The working electrode (WE), as already mentioned, a thin Au film evaporated onto a glass plate, was attached to a rectangular opening on the side wall of the cell such that the gold film was in contact with the electrolyte (cf. Fig. 3.7). The Au films were either disk shaped with a diameter of 6 mm or rectangular, in which case the area in contact with the electrolyte was 8×24 mm^2. The CE was a Pt wire bent to a circular or rectangular spiral of approximately the same geometry as the respective WE. It was aligned parallel to the WE to ensure a minimum distortion of the electric field in the electrolyte, since the latter has an important impact on pattern formation. The same is true for the distance between the CE and the WE electrode as well as for the position of the reference electrode [36, 51]. The distance between WE and CE was approx. 5 cm, and the RE was – unless stated

otherwise – located behind the CE. The argon inlet was in the center of the cell. A mercury/mercury sulfate ($Hg/Hg_2SO_4/K_2SO_4$ (sat.)) served as RE. All potentials are given with respect to this reference electrode.

The purity of the cell was of great importance in our experiments. Hence, much care was taken to clean the cell thoroughly, which was done in the following way. After rinsing the cell as well as all other parts made of glass (gas in- and outlet tubes and the counter electrode) with deionized water, they were put into a conc. nitric acid steam bath for 7–10 hours (to oxidize all the organic contamination). Subsequently, the cell and the other parts were first rinsed with Milli-Q water and then kept in a beaker filled with Milli-Q water for some time to remove the remaining traces of nitric acid. Immediately before starting the experiment, all parts were rinsed again with Milli-Q water.

3.2.2 Preparation and characterization of the working electrode

The working electrodes used in our experiments are 50 nm thick (disk shaped or rectangular) Au(111) film electrodes on a glass plate (B270, Schott, for further details see 3.2.1). The Au was evaporated onto the glass plates (10^{-6} torr and 603 K), which were beforehand covered by a 2 nm Cr layer to improve the adhesion of Au. The Cr layer had no influence on the electrochemistry [52], its effect can be neglected in the SP measurements.

Immediately before an experiment, the gold film was flame annealed. That flame annealing of thin polycrystalline Au films on quartz or glass can result in a (111) texture had been shown by Zei et al. [53]. As demonstrated by Kolb's group, it usually results in a reconstructed surface [54]. For the annealing we used a pure butane flame, through which the glass plate was slowly moved back and forth. The motion of the plate in the flame ensured that the film was heated evenly, and it avoided local overheating, which would result in breaking of the glass plate. In this way, the film was brought to a reddish glow for 1–2 minutes, then it was cooled in air. The procedure was repeated 4—5 times, after which it turned out that 1) the film was free from organic contaminants (as tested with a water droplet: the clean surface is hydrophobic, thus the droplet spreads, whereas it

has a steep contact angle if some contaminants remained on the surface) and 2) it had a high degree of (111) terraces (as apparent from CVs in $HClO_4$, see, Fig. 3.9).

The quality of the gold film is of greatest importance for our experiments. Certainly, a precondition was that there were no pronounced defects which could be seen by the naked eye. The advanced requirement was that after the flame annealing the Au surface should be predominantly (111) oriented. The orientation of the film can theoretically be checked by other techniques such as LEED, but different orientations also give rise to distinct CVs in certain supporting electrolytes, i.e., the different orientations have their own fingerprints. CVs of Au(111), Au(110), and Au(100) surfaces in a perchlorate/perchloric acid electrolyte taken from the literature [55] are reproduced in Fig. 3.8. A typical CV of our film Au electrode in 100 mM $HClO_4$ is shown in Fig. 3.9. A comparision with Fig. 3.8 clearly shows that the CV possesses all typical features of a Au(111) electrode but is very different from our CVs of the other two low indexed single crystalline surfaces.

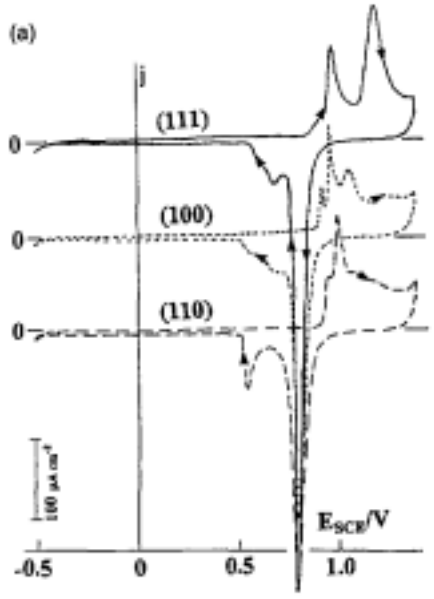

Figure 3.8: *CVs for Au(111), Au(110), Au(100) in 90 mM $NaClO_4$ + 10 mM $HClO_4$ at 25 ± 2 ℃, 50 mV/s [55].*

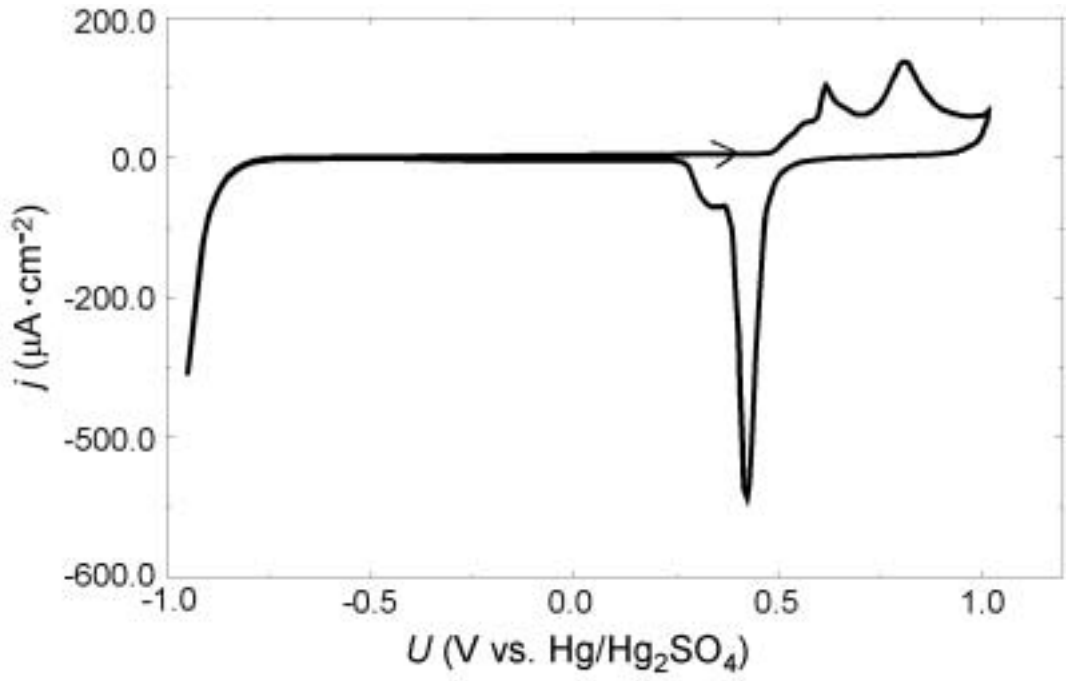

Figure 3.9: *The CV of Au(111) film electrode in 0.1 mM $HClO_4$.*

3.2.3 Electrolytes

All electrolytes were prepared from high-purity water (Milli-Q, millipore) and p.a. grade chemicals, which were used as received (Camphor: Sigma approx. 99 %; thymine: Merck, approx. 99 %; coumarin: Aros Organics, 99 %+; $Fe_3[Fe(CN)_6]$: > 99 %, Aldrich; $K_4[Fe(CN)_6]$: > 99 %, Aldrich; $NaIO_4$: Merck; $NaClO_4$, monohydrate, Merck; $Na_2S_2O_8$: Merck; H_2O_2: 30 %, Merck; $HClO_4$: 70 %, Merck; $Ru(NH_3)_6$: Merck).

In all experiments a wash bottle filled with water or the corresponding electrolyte was inserted between the gas bottle and the electrochemical cell. This arrangement, on one side, can avoid the argon gas to burst in the cell; on the other hand, it can avoid the changing of the electrolyte concentration in the cell (argon flow through the cell will bring out some components from the electrolyte). In this way, concentration changes due to the steady argon flow through the cell were minimized. This was especially important in the case of

camphor since camphor is a volatile substance. The electrolyte solutions containing camphor were prepared by dissolving the salt in a 5 mM camphor solution[1]. (Since the solubility of camphor is low，5 mM is close to the saturation concentration such that the electrolyte could not be prepared from higher concentrated solutions.)

Summary

This chapter introduced the main experimental methods employed in this thesis: After a short introduction to the principle of SPR, the two modes, in which it was employed, were discussed: SPRA measurements, used for temporal in-situ analysis of the electrochemical interface, and SPI for spatio-temporal studies of lateral potential and adsorbate distributions. Furthermore, a detailed description of the cell as well as of the preparation of the electrode and the electrolytes was given.

[1] Since camphor only badly dissolves in water, the preparation of the 5 mM camphor solution took 1–2 days during which the solution was shaken from time to time. An ultrasonic bath treatment was avoided in order to exclude chemical modifications or the formation of agglomerates.